Packet Access Using DS-CDMA With Frequency-Domain Equalization

Deepshikha Garg and Fumiyuki Adachi, *Fellow, IEEE*

***Abstract*—The next-generation mobile communications system is anticipated to support very high-speed data rates exceeding several tens megabits per second. In this paper, we consider high-speed downlink packet access for direct-sequence code-division multiple access (DS-CDMA) as in third–generation wideband code-division multiple-access systems. Adaptive modulation and coding (AMC), multicode operation and hybrid automatic repeat request (HARQ) will be the enabling technologies. With such high-speed data transmissions, however, multicode operation severely suffers from the loss of orthogonality among the spreading codes since the wireless channel becomes severely frequency-selective. In this paper, we apply frequency-domain equalization (FDE) based on minimum mean-square error (MMSE) criterion instead of conventional rake combining for receiving the packet. A new MMSE-FDE weight is derived for packet combining. The throughput in a frequency-selective Rayleigh-fading channel is evaluated by computer simulation for Chase combining and incremental redundancy (IR) packet combining. It is shown that the use of MMSE-FDE for the reception of multicode DS-CDMA packet gives an improved throughput irrespective of the channel's frequency-selectivity.**

***Index Terms*—Adaptive modulation coding (AMC), automatic repeat request, direct-sequence code-division multiple access (DS-CDMA), equalizers, error correction coding, hybrid automatic repeat request (HARQ), high-speed downlink packet access (HSDPA), minimum mean-square error frequency-domain equalization (MMSE-FDE), mobile communication, multicode.**

I. Introduction

THIRD-GENERATION (3G) mobile communications networks based on direct-sequence code-division multiple access (DS-CDMA) [1] have been successfully launched. Data services, as anticipated, have become the dominating source of traffic load in the 3G networks. High-speed data services will be supported by the high-speed downlink packet access (HSDPA) technique [2], which allows peak data rates up to around 10 Mb/s. Adaptive modulation and coding (AMC), multicode operation, and hybrid automatic repeat request (HARQ) are the enabling technologies used for HSDPA. The conventional DS-CDMA receivers consist of a rake combiner that can take advantage of the path diversity. The next-generation mobile communications system is anticipated to support even higher data rates exceeding several tens Mb/s [3]. With such high-speed data transmissions, the wireless channel becomes severely frequency-selective [4]. However, when the number of propagation paths in the channel increases, the receiver complexity increases due to the increase in the number of rake fingers. Moreover, in a frequency-selective channel, multicode operation severely suffers from the loss of orthogonality among the orthogonal spreading codes and the performance with coherent Rake combining severely degrades.

AMC will still be important for the next-generation mobile communications systems to benefit from the time-varying channel conditions. The use of multilevel modulation and multicode operation supports high-speed transmissions. However, recent standards like HSDPA use Rake combining that is not suitable for high-level modulations and multicode operation over frequency-selective channels. Hence, it is important to use other techniques suitable for multicode operation and also multilevel modulation over frequency-selective channels. Various time-domain and frequency-domain equalization techniques [5]–[12] have been proposed to improve the DS-CDMA transmission performance.

Recently, it was shown [7]–[9] that DS-CDMA using frequency-domain equalization based on minimum mean-square error criterion (MMSE-FDE) can partially restore the orthogonality and provide a better bit-error rate (BER) performance than conventional Rake combining. In [7], it is shown that the BER performance of multicode DS-CDMA with MMSE-FDE improves with the increase in the frequency-selectivity of the channel. The throughput improves because of orthogonality restoration to a certain extent. MMSE-FDE is an equalization that minimizes the error in frequency-domain between the equalized received signal and the transmitted signal. Other commonly used frequency-domain equalization methods are zero forcing (ZF) and maximum ratio combining (MRC). MRC in the frequency-domain is equivalent to the Rake combining in time-domain. However, it has been shown in [8] that MMSE-FDE provides the best performance.

For packet transmissions, the frequency-selectivity of the channel is not always desirable. With higher frequency-selectivity, the bit errors are randomized; however, burst nature of bit errors is preferable to random nature of bit errors for packet transmissions. Hence, there is a need to evaluate the performance of packet transmissions in a frequency-selective channel. In [7] and [8], the BER of an uncoded DS-CDMA system with MMSE-FDE is evaluated for quadrature phase-shift keying (QPSK) data modulation. The BER performance for 16 quadrature amplitude modulation (QAM) data modulation is evaluated in [9], but error correction coding has not been considered. In

Manuscript received September 22, 2005; revised May 31, 2005. Part of this work was presented at IEEE VTC04 Fall.

D. Garg was with the Department of Electrical and Communications Engineering, Tohoku University, Sendai, Japan. She is now with Kyocera Telecommunications Research Corporation, San Jose, CA 95131 USA (e-mail: dgarg@ktrc-na.com).

F. Adachi is with the Department of Electrical and Communications Engineering, Tohoku University, Sendai 980-8579, Japan (e-mail: adachi@ecei. tohoku.ac.jp).

Digital Object Identifier 10.1109/JSAC.2005.858899

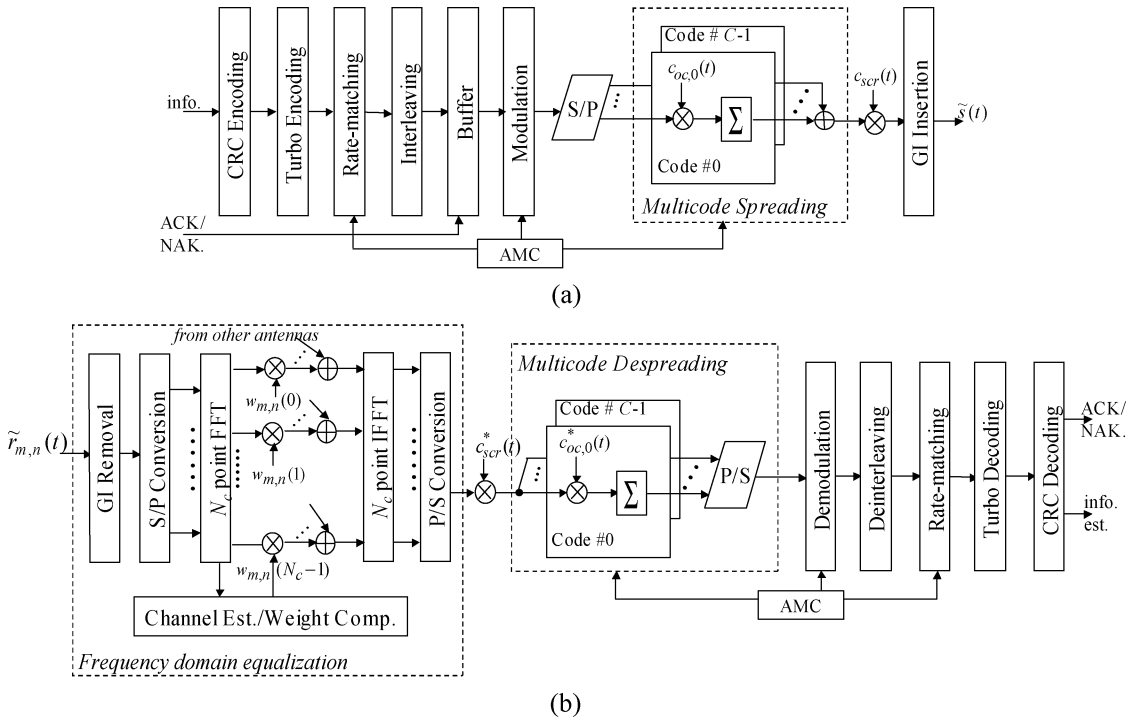

Fig. 1. Transmission system model with MMSE-FDE at the receiver. (a) Transmitter. (b) Receiver.

addition, the packet transmission performance has not been evaluated. In [10]–[12], different equalizers for DS-CDMA are compared and concluded that FDE is better than time-domain equalization (TDE). In [11], it is concluded that FDE is much simpler than TDE due to frequency-domain processing. In [12], TDE and FDE are compared in terms of the complexity, and it is shown that FDE has the lowest complexity, with even fewer multiplications than the Rake combining. Hence, in this paper, we concentrate on the FDE.

With packet transmissions, AMC and HARQ are very important for error control. In this paper, we incorporate MMSE-FDE to packet transmissions with AMC and HARQ. We consider HARQ schemes using both Chase combining (CC) [13] and incremental redundancy (IR) [14]. In CC, the retransmitted packets are combined to benefit from the time diversity gain [15] as in antenna diversity to increase the received signal power. In IR, the redundancy is increased with each retransmission, resulting in a decreased coding rate and, thus, a better error correction capability. A new MMSE-FDE weight is derived for frequency-domain packet combining and the packet throughput is evaluated under full load conditions over a severe frequency-selective channel.

The remainder of this paper is organized as follows. Section II describes the DS-CDMA high-speed downlink packet access with MMSE-FDE. The MMSE weight for packet combining is also introduced. The simulation results are presented and discussed in Section III. The performance of DS-CDMA downlink packet access with MMSE-FDE is compared with that of the nonspread single carrier transmission [16], [17]. In addition, the Shannon limit for a frequency-selective Rayleigh-fading channel is presented and the throughput achieved for DS-CDMA with AMC, HARQ and multicode operation is compared with the Shannon limit. Also, the throughput is compared with that of multicarrier CDMA (MC-CDMA). Section IV concludes this paper.

II. Packet Access for DS-CDMA With FDE

The conventional DS-CDMA receivers are equipped with a Rake combiner that coherently combines the signals arrived over different paths and takes advantage of the path diversity. When the number of propagation paths in the channel increases, the receiver complexity increases due to the increase in the number of Rake fingers. In addition, in a frequency-selective channel, the orthogonality among the orthogonal spreading codes is distorted due to severe interpath interference and, therefore, multicode operation cannot guarantee high-speed transmissions. However, the orthogonality can be partially restored with MMSE-FDE and, hence, MMSE-FDE is suitable for multicode operation. In this paper, we propose the use of MMSE-FDE for the reception of multicode packet signals.

A. Overall Packet Transmission System Model

The transmitter and receiver for DS-CDMA packet access with MMSE-FDE are shown in Fig. 1. Guard interval (GI) insertion block, which is not present in the current DS-CDMA receivers, is added at the transmitter. The receiver structure is modified to incorporate the FDE; fast Fourier transform (FFT) and inverse FFT (IFFT) blocks are added and the Rake combiner is removed.

Similar to HSDPA, we consider the multicode transmission with the spreading factor SF. HARQ with CC (single redundancy version) [13] or IR (each retransmission may use a different redundancy version) [14] may be used. With FDE, the received packet signal is first converted to frequency components by FFT and MMSE equalization is performed for

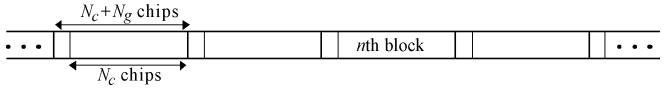

Fig. 2. Frame structure for DS-CDMA with MMSE-FDE.

each frequency component, after which the frequency-domain signal is transformed back to time-domain signal by IFFT. However, with FDE, it is essential that the signal be periodic in the FFT window and, hence, GI in the form of cyclic prefix needs to be inserted [7]–[12] in the transmit signal as for MC-CDMA. At the transmitter, rate matching [2] can be modified so as to allow for GI insertion.

B. Transmit and Receive Signal Representation

The binary information sequence is first turbo coded and punctured according to the channel quality indicator (CQI). It is then interleaved and modulated according to CQI. We consider the transmission of the data-modulated symbol sequence $\{x_c(i); i = 0 \sim K-1\}$. Orthogonal multicode spreading is performed on $\{x_c(i)\}$. In this paper, chip-spaced discrete-time representation of signals is used. The resulting multicode DS-CDMA signal can be expressed, using the equivalent low-pass representation, as

$$s(t) = \sqrt{\frac{2P}{\mathrm{SF}}} \sum_{c=0}^{C-1} x_c\left(\left\lfloor \frac{t}{\mathrm{SF}} \right\rfloor\right) c_{oc,c}(t \bmod \mathrm{SF}) c_{\mathrm{scr}}(t) \quad (1)$$

for $t = 0 \sim \mathrm{SF} \cdot K - 1$, where P represents the transmit power per code, $c_{oc,c}(t)$ and $c_{\mathrm{scr}}(t)$ are, respectively, the channelization code and the common scrambling code with $|c_{oc,c}(t)| = |c_{\mathrm{scr}}(t)| = 1$, SF is the spreading factor, $C(\leq \mathrm{SF})$ is the number of codes multiplexed, and $\lfloor x \rfloor$ represents the largest integer smaller than or equal to x. In (1), $E[x_c(i)^2] = 1$ is assumed, where $E[.]$ denotes the ensemble average operation. The orthogonal spreading codes and the scrambling code have the following characteristics:

$$\begin{cases} \frac{1}{\mathrm{SF}} \sum_{t=0}^{\mathrm{SF}-1} c_{oc,c}(t) c^*_{oc,c'}(t) = \delta(c - c') \\ E\left[c_{\mathrm{scr}}(t) c^*_{\mathrm{scr}}(\tau)\right] = \delta(t - \tau) \end{cases} \quad (2)$$

where $(.)^*$ denotes the complex conjugate operation and $\delta(.)$ the delta function.

N_g-chip GI is inserted for every block of N_c chips; N_c is the number of FFT/IFFT points at the receiver and N_g is a fraction of N_c. The resulting GI-inserted multicode DS-CDMA signal $\widetilde{s}(t)$ is transmitted over the propagation channel. The transmitted signal frame structure is shown in Fig. 2. Compared with Rake combining, there is a loss in the data rate by a factor of $(1+N_g/N_c)$ due to the GI needed when MMSE-FDE is used.

A chip-spaced time delay model for the propagation channel is assumed. M-branch antenna diversity reception is considered. Assuming L independent propagation paths with distinct time delays $\{\tau_l; l = 0 \sim L-1\}$, the impulse response $h_{m,n}(\tau)$ of the multipath channel for the mth antenna, $m = 0 \sim M-1$, for the nth block of $N_c + N_g$ chips, can be expressed as

$$h_{m,n}(\tau) = \sum_{l=0}^{L-1} \xi_{m,n,l} \delta(\tau - \tau_l) \quad (3)$$

with $\sum_{l=0}^{L-1} \mathrm{E}[|\xi_{m,n,l}|^2] = 1$, where $\xi_{m,n,l}$ is the complex-valued path gain of the lth path. We have assumed block fading where the path gains stay constant over a duration of at least one block. The received multicode DS-CDMA signal is sampled at the chip rate; the nth block chip sequence $\widetilde{r}_{m,n}(t)$ of $N_c + N_g$ chips can be expressed as

$$\widetilde{r}_{m,n}(t) = \sum_{l=0}^{L-1} \xi_{m,n,l} \widetilde{s}(t - \tau_l) + \eta_{m,n}(t) \quad (4)$$

where $\eta_{m,n}(t)$ is the zero-mean Gaussian process with variance $2N_0/T_c$ due to the additive white Gaussian noise (AWGN) having the one-sided power spectrum density N_0; T_c is the chip length. Ideal sampling timing is assumed. The N_g-sample GI is removed and N_c-point FFT is applied to each block of N_c chips in order to decompose the received multicode DS-CDMA signal into the N_c frequency components. The kth frequency component for the nth block is

$$\begin{aligned} R_{m,n}(k) &= \sum_{t=0}^{N_c-1} \widetilde{r}_{m,n}(t) \exp\left(-\frac{j2\pi kt}{N_c}\right) \\ &= H_{m,n}(k) S_n(k) + \Pi_{m,n}(k) \end{aligned} \quad (5)$$

for $k = 0 \sim N_c - 1$ and $n = 0 \sim \mathrm{SF}(K/N_c) - 1$, where $H_{m,n}(k)$ and $\Pi_{m,n}(k)$, respectively, denote the channel gain and the noise component due to the AWGN at the kth frequency component in the nth block for the mth receive antenna and $S_n(k)$ is the Fourier transform of the nth block of the transmitted multicode DS-CDMA signal, and are given by

$$\begin{cases} S_n(k) = \sum_{t=nN_c}^{(n+1)N_c-1} s(t) \exp\left(-j2\pi t \frac{k}{N_c}\right) \\ H_{m,n}(k) = \sum_{l=0}^{L-1} \xi_{m,n,l} \exp\left(-j2\pi k \frac{\tau_l}{N_c}\right) \\ \Pi_{m,n}(k) = \sum_{t=0}^{N_c-1} \eta_{m,n}(t) \exp\left(-j2\pi k \frac{t}{N_c}\right). \end{cases} \quad (6)$$

C. MMSE-FDE

In this paper, we introduce MMSE weights for frequency-domain packet combining. Joint MMSE-FDE and antenna diversity combining is carried out using the equalization weight $w_{m,n}(k)$ for $R_{m,n}(k)$ as

$$\widetilde{R}_n(k) = \sum_{m=0}^{M-1} w_{m,n}(k) R_{m,n}(k). \quad (7)$$

The weights are chosen to minimize the error between $\widetilde{R}_n(k)$ and $S_n(k)$. For IR, the retransmitted packet consists of different symbols and $w_{m,n}(k)$ is taken to be [8]

$$w_{m,n}(k) = \frac{H^*_{m,n}(k)}{\sum_{m=0}^{M-1} |H_{m,n}(k)|^2 + \left[\frac{C}{\mathrm{SF}} \frac{E_s}{N_0}\right]^{-1}} \quad (8)$$

where $E_s = PT_s$ is the average received symbol energy.

When CC is employed, the same packet is retransmitted, time diversity gain can be obtained since multiple copies of the same packet are combined as

$$\widetilde{R}_n(k) = \sum_{tr=0}^{Tr_{\max}-1} \sum_{m=0}^{M-1} w_{m,n,tr}(k) R_{m,n,tr}(k) \tag{9}$$

where $Tr_{\max}$ is the number of times the same packet is received, $w_{m,n,tr}(k)$, and $R_{m,n,tr}(k)$ are the MMSE-FDE weight and the received signal for the trth transmission, respectively. Equation (9) is equivalent to $M \times Tr_{\max}$-branch antenna diversity reception and, hence, the MMSE-FDE weight for frequency-domain packet combining is modified as

$$w_{m,n,tr}(k) = \frac{H^*_{m,n,tr}(k)}{\sum_{tr=0}^{Tr_{\max}-1} \sum_{m=0}^{M-1} |H_{m,n,tr}(k)|^2 + \left[\frac{C}{\mathrm{SF}} \frac{E_s}{N_0}\right]^{-1}} \tag{10}$$

where $H_{m,n,tr}(k)$ is the value of $H_{m,n}(k)$ at the trth transmission.

After performing MMSE-FDE, N_c-point IFFT is carried out to obtain the multicode DS-CDMA signal in the time-domain

$$\begin{aligned}\hat{s}(t) &= \frac{1}{N_c} \sum_{k=0}^{N_c-1} \widetilde{R}_n(k) \exp\left(\frac{j2\pi kt}{N_c}\right) \\ &= \frac{1}{N_c} \left\{ s(t) \sum_{k=0}^{N_c-1} \widetilde{H}_n(k) + \sum_{k=0}^{N_c-1} \widetilde{H}_n(k) \right. \\ &\qquad \left. \times \sum_{\substack{\tau=0 \\ \neq t}}^{N_c-1} s(\tau) \exp\left(j2\pi(t-\tau)\frac{k}{N_c}\right) \right\} \\ &\quad + \widetilde{\eta}_n(t)\end{aligned} \tag{11}$$

where $n = \lfloor t/N_c \rfloor$, and $\widetilde{H}_n(k)$ and $\widetilde{\eta}_n(t)$ are as shown in (12) at the bottom of the page. In (12b), $\Pi_{m,n,tr}(k)$ is the noise component of the received packet for the trth transmission. IFFT is followed by multicode despreading to obtain

$$\begin{aligned}\hat{x}_c(i) &= \sum_{t=i\mathrm{SF}}^{(i+1)\mathrm{SF}-1} \hat{s}(t) \{c_{oc,c}(t \bmod \mathrm{SF}) c_{\mathrm{scr}}(t)\}^* \\ &= \sqrt{\frac{2P}{\mathrm{SF}}} \left(\frac{1}{N_c} \sum_{k=0}^{N_c-1} \widetilde{H}_n(k)\right) x_c(i) \\ &\quad + \mu_{\mathrm{ICI}}(i) + \mu_{\mathrm{noise}}(i)\end{aligned} \tag{13}$$

for $c = 0 \sim C-1$ and $i = 0 \sim K-1$. In (13), the first term represents the desired data symbol component and the second and third terms, $\mu_{ICI}(t)$ and $\mu_{\mathrm{noise}}(t)$, are interchip interference (ICI) and the noise due to AWGN, respectively, given by

$$\begin{cases} \mu_{\mathrm{ICI}}(i) = \frac{1}{\mathrm{SF}} \sum_{t=i\mathrm{SF}}^{(i+1)\mathrm{SF}-1} \{c_{oc,c}(t \bmod \mathrm{SF}) c_{\mathrm{scr}}(t)\}^* \\ \quad \times \frac{1}{N_c} \sum_{k=0}^{N_c-1} \widetilde{H}_n(k) \left[\sum_{\substack{\tau=0 \\ \neq t}}^{N_c-1} s(\tau) \exp\left(j2\pi k \frac{t-\tau}{N_c}\right)\right] \\ \mu_{\mathrm{noise}}(i) = \frac{1}{\mathrm{SF}} \sum_{t=i\mathrm{SF}}^{(i+1)\mathrm{SF}-1} \{c_{oc,c}(t \bmod \mathrm{SF}) c_{\mathrm{scr}}(t)\}^* \widetilde{\eta}_n(t) \end{cases} \tag{14}$$

It can be understood from (13) that $\hat{H}_n(i) = (1/N_c) \sum_{k=0}^{N_c-1} \widetilde{H}_n(k)$ can be considered as the equivalent channel gain for all the symbols within the nth FFT block and the frequency diversity gain is not a function of SF. $\{\hat{x}_c(i); c = 0 \sim C-1\}$ are parallel-to-serial (P/S) converted for data demodulation.

D. Log-Likelihood Ratio (LLR) for Turbo Decoding

The soft decision values for turbo decoding are generated using the LLR [18]. We assume that ICI can be approximated as a complex Gaussian noise and, therefore, we treat the sum of ICI and noise as a new complex Gaussian noise process with variance $2\sigma^2$. The LLR is given by

$$L(b) = \ln\left[\frac{\sum_{\{\hat{s}:b=1\}} \frac{1}{\sqrt{2\pi\sigma^2}} \exp\left(-\frac{1}{2\sigma^2}\left|\hat{x}_c(i) - \sqrt{\frac{2P}{\mathrm{SF}}}\hat{H}_n(i)\hat{s}\right|^2\right)}{\sum_{\{\hat{s}:b=0\}} \frac{1}{\sqrt{2\pi\sigma^2}} \exp\left(-\frac{1}{2\sigma^2}\left|\hat{x}_c(i) - \sqrt{\frac{2P}{\mathrm{SF}}}\hat{H}_n(i)\hat{s}\right|^2\right)}\right] \tag{15}$$

where $\hat{s}$ is the candidate symbol with the bth bit as 0 or 1; $b = 0 \sim B-1$ with $B = 2$, 4, or 6 for QPSK, 16 and 64 QAM, respectively. The variance $2\sigma^2$ of the Gaussian approximated ICI plus noise is given by [19]

$$\begin{aligned}2\sigma^2 &= \frac{2}{\mathrm{SF}} \frac{N_0}{T_s} \\ &\quad \times \left[\begin{array}{l} \frac{1}{N_c} \sum_{k=0}^{N_c-1} \sum_{m=0}^{M-1} |w_{m,n}(k)|^2 + \left(\frac{C}{\mathrm{SF}} \frac{PT_s}{N_0}\right) \\ \times \left\{ \frac{1}{N_c} \sum_{k=0}^{N_c-1} \left|\widetilde{H}_n(k)\right|^2 - \left|\frac{1}{N_c} \sum_{k=0}^{N_c-1} \widetilde{H}_n(k)\right|^2 \right\} \end{array}\right]\end{aligned} \tag{16}$$

for IR. For CC, $|w_{m,n}(k)|^2$ in (16) is replaced by $\sum_{tr=0}^{Tr_{\max}-1} |w_{m,n,tr}(k)|^2$.

$$\widetilde{H}_n(k) = \begin{cases} \sum_{m=0}^{M-1} w_{m,n}(k) H_{m,n}(k), & \text{for IR} \\ \sum_{tr=0}^{Tr_{\max}-1} \sum_{m=0}^{M-1} w_{m,n,tr(k)} H_{m,n,tr}(k), & \text{for CC} \end{cases} \tag{12a}$$

$$\widetilde{\eta}_n(t) = \begin{cases} \frac{1}{N_c} \sum_{k=0}^{N_c-1} \left\{ \sum_{m=0}^{M-1} w_{m,n}(k) \Pi_{m,n}(k) \right\} \exp\left(j2\pi k \frac{t}{N_c}\right), & \text{for IR} \\ \frac{1}{N_c} \sum_{k=0}^{N_c-1} \left\{ \sum_{tr=0}^{Tr_{\max}-1} \sum_{m=0}^{M-1} w_{m,n,tr}(k) \Pi_{m,n,tr}(k) \right\} \exp\left(j2\pi k \frac{t}{N_c}\right), & \text{for CC} \end{cases} \tag{12b}$$

From [18], we approximate the denominator and numerator inside the brackets of (15) as

$$\sum_{\{\hat{s}:b=1 \text{ or } 0\}} \frac{1}{\sqrt{2\pi\sigma^2}} \exp\left(-\frac{1}{2\sigma^2}\left|\hat{x}_c(i) - \sqrt{\frac{2P}{\mathrm{SF}}}\hat{H}_n(i)\hat{s}\right|^2\right) \approx \max_{\{\hat{s}:b=1 \text{ or } 0\}} \frac{1}{\sqrt{2\pi\sigma^2}} \times \exp\left(-\frac{1}{2\sigma^2}\left|\hat{x}_c(i) - \sqrt{\frac{2P}{\mathrm{SF}}}\hat{H}_n(i)\hat{s}\right|^2\right). \quad (17)$$

Representing

$$\max_{\{\hat{s}:b=1 \text{ or } 0\}} \frac{1}{\sqrt{2\pi\sigma^2}} \exp\left(-\frac{1}{2\sigma^2}\left|\hat{x}_c(i) - \sqrt{\frac{2P}{\mathrm{SF}}}\hat{H}_n(i)\hat{s}\right|^2\right) = \frac{1}{\sqrt{2\pi\sigma^2}} \times \exp\left(-\frac{1}{2\sigma^2}\left|\hat{x}_c(i) - \sqrt{\frac{2P}{\mathrm{SF}}}\hat{H}_n(i)\hat{s}_{1 \text{ or } 0,\max}\right|^2\right) \quad (18)$$

the LLR can be written as

$$L(b) = \frac{1}{2\sigma^2}\left(\left|\hat{x}_c(i) - \sqrt{\frac{2P}{\mathrm{SF}}}\hat{H}_n(i)\hat{s}_{0,\max}\right|^2 - \left|\hat{x}_c(i) - \sqrt{\frac{2P}{\mathrm{SF}}}\hat{H}_n(i)\hat{s}_{1,\max}\right|^2\right) \quad (19)$$

for the bth bit in the ith symbol. The LLR values are computed for $c = 0 \sim C-1$ and for all the bits in the symbol. Turbo decoding is performed using these LLR values as soft input after rate matching. Then, error detection is performed and retransmission is requested if errors are detected.

III. Simulation Results

The simulation conditions are summarized in Table I. For the simulation purpose, we assume a frequency-selective block Rayleigh-fading channel having a chip-spaced L-path uniform power delay profile and a normalized maximum Doppler frequency $f_D T_{\mathrm{blk}}$ of 0.001, where f_D is the maximum Doppler frequency given by terminal traveling speed/carrier wavelength, and T_{blk} is the block length with $N_c + N_g$ chips (i.e., $T_{\mathrm{blk}} = T_c(N_c + N_g)$). In the simulation, $N_c = 256$ and $N_g = 32$ are assumed. The Walsh–Hadamard codes are used as channelization codes $\{c_{oc,c}(t); t = 0 \sim \mathrm{SF}-1, c = 0 \sim \mathrm{SF}-1\}$. Code multiplexing of $C = \mathrm{SF}$ is assumed that provides the same data rate as the nonspread single carrier modulation [16], [17]. $C = \mathrm{SF} = 16$ is assumed unless otherwise stated. Long pseudonoise code sequence is used as scrambling code.

In AMC, a rate-1/3 turbo code having two (13,15) recursive systematic convolutional (RSC) encoders same as in HSDPA, with the rate R varied between 1/2 and 3/4, and QPSK, 16 and 64 QAM are used, as shown in Table II. Ideal AMC is assumed, i.e., the modulation and coding rate set (MCS) that gives the highest performance at each average received signal energy per symbol-to-the noise power spectral density ratio (E_s/N_0) is selected, and it is assumed that there is no selection error.

TABLE I
Simulation Conditions

Turbo coding	R=1/2 and 3/4 (13, 15) RSC encoder Log-MAP decoding with 8 iterations	
Channel interleaver	Block interleaver	
Data modulation	Coherent QPSK, 16QAM, 64QAM	
DS-CDMA	No. of FFT points	N_c=256
	GI	N_g=32
	Spreading factor	SF=16
ARQ	Incremental redundancy/ Chase combining	
Channel model	L-path block Rayleigh fading $\tau_l = l$, $f_D T_{blk}$=0.001	

TABLE II
Modulation and Coding Rate Set

MCS	Modulation	Coding rate R	Information bits/symbol
1	QPSK	½	1
2	QPSK	¾	1.5
3	16QAM	½	2
4	16QAM	¾	3
5	64QAM	½	3
6	64QAM	¾	4.5

TABLE III
Puncturing Pattern

R	½	¾
P_1	$\begin{bmatrix}1&1\\1&0\\0&1\end{bmatrix}$	$\begin{bmatrix}1&1&1&1&1&1\\1&0&0&0&0&0\\0&0&0&1&0&0\end{bmatrix}$
P_2	$\begin{bmatrix}1&1\\0&1\\1&0\end{bmatrix}$	$\begin{bmatrix}0&0&0&0&0&0\\0&1&1&1&1&0\\1&1&0&0&1&1\end{bmatrix}$

The puncturing matrices are shown in Table III. For CC, the same packet with puncturing matrix P_1 is transmitted until a positive acknowledgment is received. For IR, the puncturing matrix P_1 is used for the first transmission and P_2 for the second transmission [20] and the order repeated for further transmissions. Code combining is employed if the same packet is transmitted more than once. Ideal chip synchronization and ideal channel estimation are assumed at the receiver. Perfect error detection and an error-free feedback channel are assumed. The number of retransmissions is assumed to be unlimited.

The throughput performance with Rake combining is presented first. It is shown how the throughput with Rake combining is affected by the frequency-selectivity of the channel. Then, it is shown that the use of MMSE-FDE can maintain a high throughput irrespective of the channel's frequency-selectivity. The throughput is compared with that of Rake combining. The

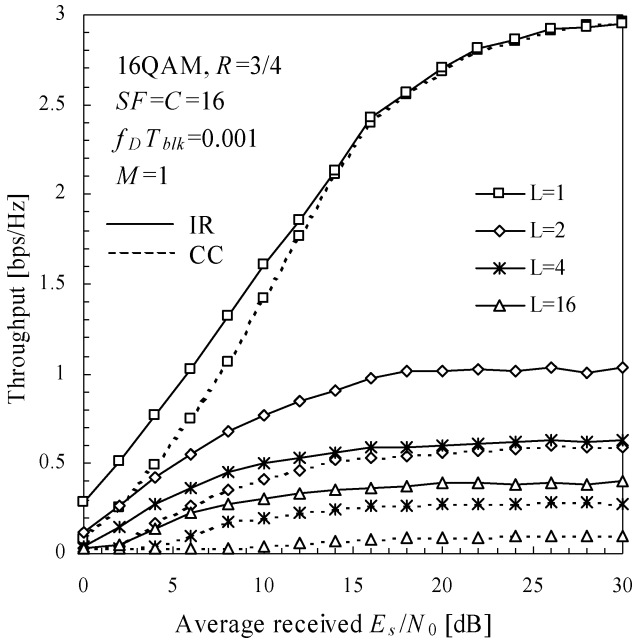

Fig. 3. Throughput with Rake combing for $R = 3/4$ and 16 QAM.

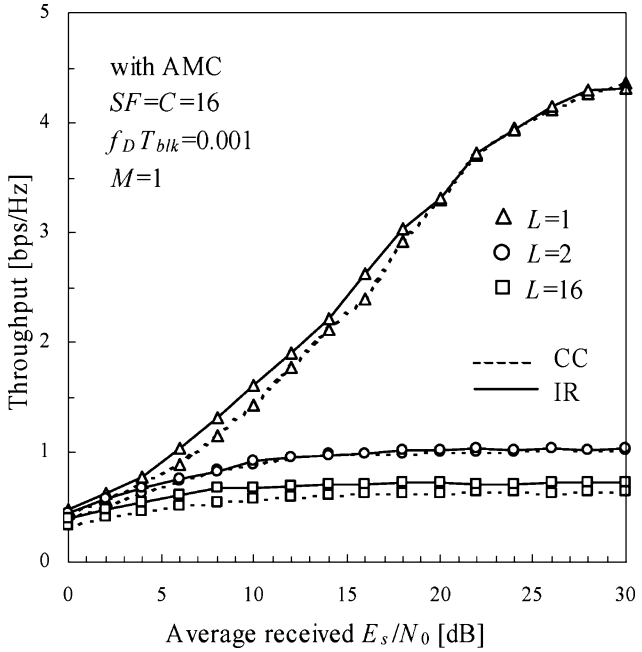

Fig. 4. Throughput with Rake combing for AMC.

improvement in throughput with antenna diversity reception is also shown. Finally, we compare the throughput with that of nonspread single carrier system. Also, the throughput is compared with that of MC-CDMA systems.

In this paper, the throughput is given in bits per second per Hertz (b/s/Hz) and the throughput in b/s can be obtained if the bandwidth is given. However, it should be noted that as the bandwidth increases, the channel frequency-selectivity may become stronger since the number L of resolvable paths increases; therefore, the MMSE-FDE may have a larger advantage over Rake combining.

A. Rake Combining

Conventional receivers have a Rake combiner. Here, we assume that the number of fingers in the Rake combiner is the same as the number L of resolvable paths in the channel. Fig. 3 plots the throughput in b/s/Hz as a function of the average received E_s/N_0 for $R = 3/4$ and 16 QAM with L as a parameter when Rake combining is used at the receiver. The modulation and coding rate is fixed to concentrate on the effect of L. $C = \mathrm{SF} = 16$ is assumed. It is seen that for both CC and IR, the throughput degrades drastically when L increases. For $L = 1$, the throughput gradually increases with the increase in the average received E_s/N_0. However, even for $L = 2$, the throughput attainable with Rake combining is drastically reduced due to the loss of orthogonality among the spreading codes. With the increase in L, the frequency-selectivity of the channel increases and the orthogonality distortion is severer. Hence, the throughput decreases with the increase in L.

Fig. 4 plots the throughput in b/s/Hz with AMC. The MCS sets are as specified in Table II. It is seen that IR provides a slightly higher throughput than CC for all channel conditions. In IR, the second retransmission consists of the unsent parity bits instead of sending the same bits as in CC. From the result it can be inferred that the additional coding gain due to increased redundancy is more desirable than the increased received signal power owing to packet combining. However, even with AMC, the throughput decreases drastically with the increase in the frequency-selectivity of the channel.

B. MMSE-FDE

The throughput with the proposed MMSE-FDE receiver is plotted in Fig. 5(a) and (b) for CC and IR, respectively, when 16 QAM modulation and rate 3/4 turbo code is used. As for Rake combining, we first evaluate the effect of the frequency-selectivity of the channel. With Rake combining, as seen in Figs. 3 and 4, IR provides slightly higher throughput and the throughput for both IR and CC decrease as the number L of paths increases (or the channel frequency-selectivity becomes stronger). However, with MMSE-FDE, the throughput is much higher and is almost insensitive to L. This is because the code orthogonality distortion is severer for stronger frequency-selectivity; but, MMSE-FDE can partially restore the code orthogonality and, therefore, benefits from the frequency-selectivity of the channel [7], [8]. In addition, with the MMSE-FDE weight, CC and IR provide almost the same throughput.

It can be observed in Fig. 5(a) and (b), that in the low E_s/N_0 regions, the throughput is slightly better for $L = 1$, whereas it is better for $L = 16$ in the high E_s/N_0 regions. This can be explained as follows. Increased frequency-selectivity results in increasing the random nature of bit errors which are desirable for channel coding but undesirable for packet transmissions. For lower E_s/N_0 regions, the throughput is lower for frequency-selective channel $(L = 16)$ than for frequency-nonselective channel $(L = 1)$. This is because, even with MMSE-FDE, the bit errors are too many to be corrected by the turbo decoder and random which is not favorable for packet transmission. However, for higher E_s/N_0 regions, with MMSE-FDE, there are only few bit errors in a packet, that

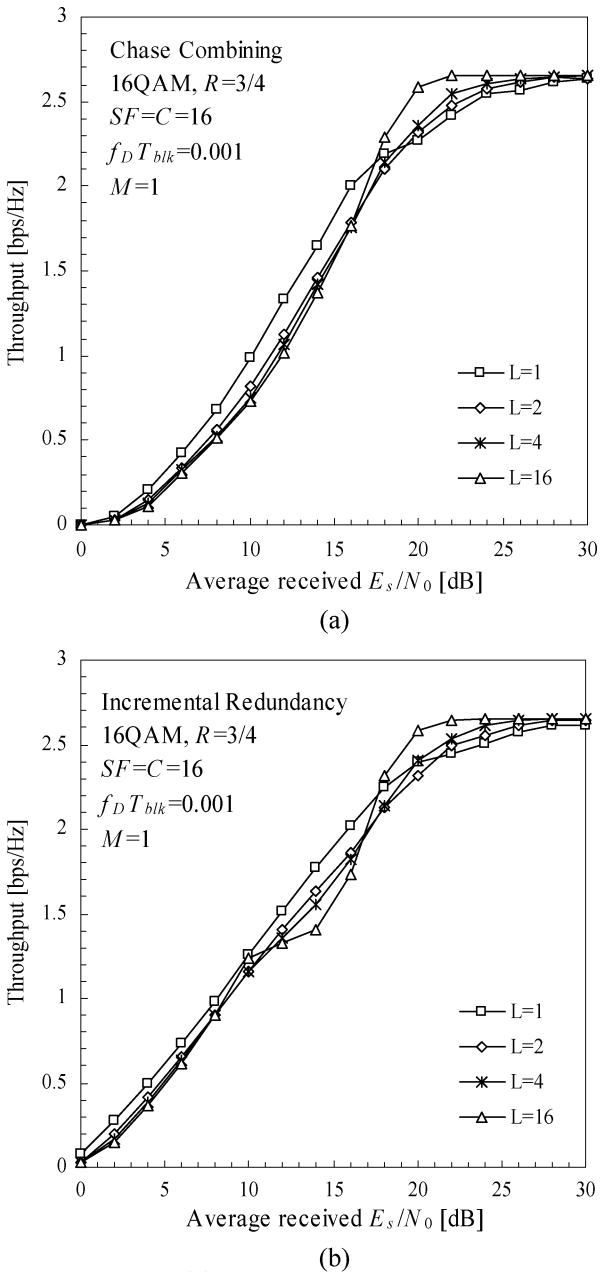

Fig. 5. Throughput with MMSE-FDE for R=3/4 and 16 QAM. (a) Chase combining. (b) Incremental redundancy.

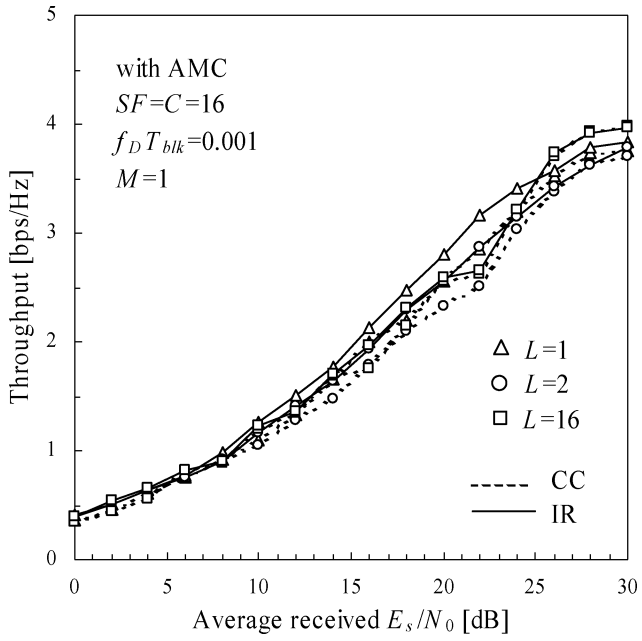

Fig. 6. Throughput for MMSE-FDE with AMC.

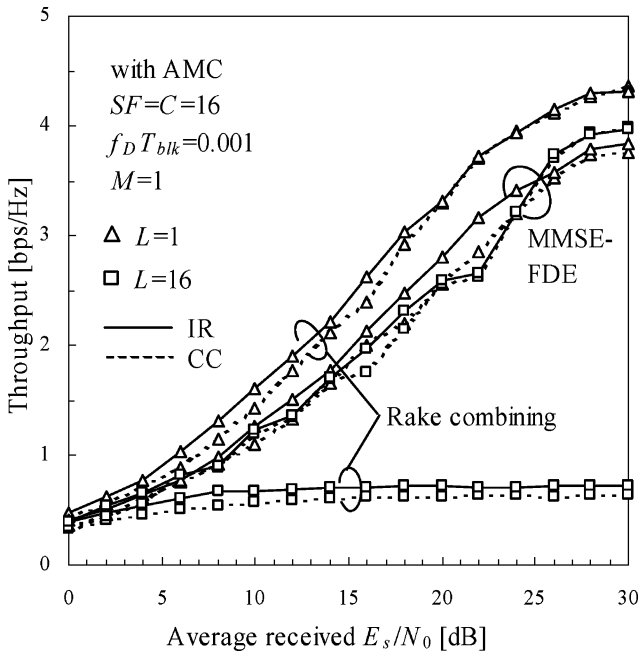

Fig. 7. Throughput comparison of MMSE-FDE and Rake combining.

can be corrected by the turbo decoder and the throughput is higher for frequency-selective channel ($L = 16$). Note that even for very high E_s/N_0 values, the maximum attainable throughput is 2.65 b/s/Hz with $R = 3/4$ and 16 QAM due to the GI insertion loss.

The throughput performance with AMC in addition to multicode operation and HARQ is plotted in Fig. 6 when MMSE-FDE is employed instead of Rake combining. Even with AMC, there is almost no difference in throughput with the increase in L. For all modulation schemes and all coding rates, MMSE-FDE can partially restore the code orthogonality, giving an improved throughput. It can also be noted that IR is only slightly better than CC employing frequency-domain packet combining.

Fig. 7 compares the throughput with MMSE-FDE and Rake combining as a function of the average received E_s/N_0 with AMC for CC and IR. For $L = 1$, the throughput is lower with MMSE-FDE compared with Rake combining, due to the GI insertion. However, for $L = 16$, the throughput is much better than that of Rake combining. Rake combining is not suitable for channels with high frequency-selectivity as the orthogonality gets severely distorted resulting in a large ICI. The MMSE-FDE provides a good tradeoff between orthogonality restoration and noise enhancement [8] and is suitable for channels with high frequency-selectivity.

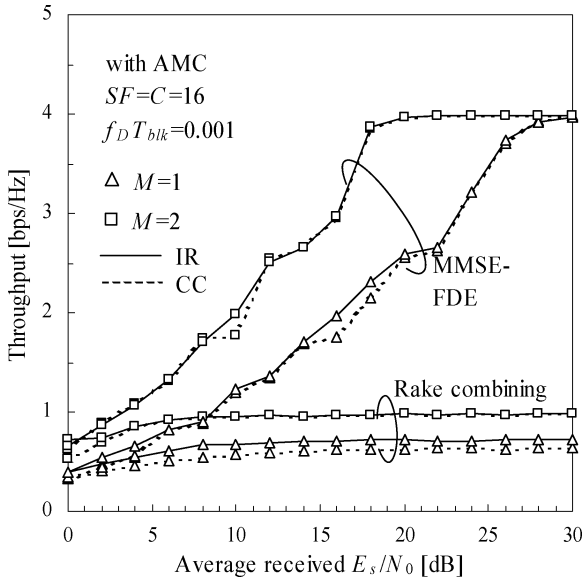

Fig. 8. Effect of antenna diversity.

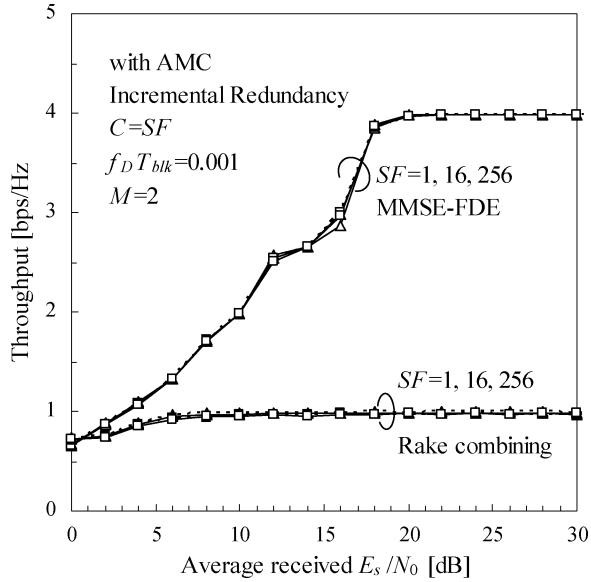

Fig. 9. Effect of spreading factor.

C. Effect of Antenna Diversity Reception

The improvement in the throughput performance with the use of two-antenna diversity reception is plotted in Fig. 8 for IR and CC when $L = 16$ and AMC is used. For both IR and CC, antenna diversity reception yields higher throughput; the throughput with MMSE-FDE is increased by about 50% for $E_b/N_0 = 20$ dB compared with the no antenna diversity case. It can be observed that even with antenna diversity reception, IR has a very small advantage over CC. The use of antenna diversity reception improves the throughput for Rake combining as well, but the achievable throughput is much smaller than that for MMSE-FDE without antenna diversity.

D. Effect of Spreading Factor

In DS-CDMA, it is possible to change the spreading factor, while keeping the same symbol rate. The IR throughput with MMSE-FDE for $\mathrm{SF} = 1$, 16, and 256 are plotted in Fig. 9 for $L = 16$ and $M = 2$ when AMC is utilized. To maintain the symbol rate fixed, $C = \mathrm{SF}$ is assumed. $\mathrm{SF} = 1$ corresponds to the nonspread single carrier transmission [16], [17]. The throughput of DS-CDMA with Rake combining is also plotted for reference. It is seen from Fig. 9 that the throughput of DS-CDMA with MMSE-FDE is independent of SF. As was discussed in Section II, the frequency diversity effect in DS-CDMA with MMSE-FDE does not depend on SF since each symbol is spread over the entire bandwidth and equalization is carried out in frequency-domain. Thus, each symbol benefits from the full frequency diversity. The amount of ICI after equalization depends on the C/SF ratio as can be seen from (16). Hence, when $C = \mathrm{SF}$, the DS-CDMA performance is the same irrespective of SF.

E. Comparison With MC-CDMA

The throughput of DS-CDMA with MMSE-FDE is compared with that of MC-CDMA. The number of subcarriers in MC-CDMA is taken to be $N_c = 256$ and the MCSs are taken to be the same as that for DS-CDMA. Fig. 10 plots the throughput in b/s/Hz for MC-CDMA and DS-CDMA both with $\mathrm{SF} = C = 256$ as a function of E_s/N_0 with AMC when $L = 16$ for IR. Since $S_F = N_c = 256$ in MC-CDMA, each data symbol is spread over the entire bandwidth and is equivalent to DS-CDMA. Hence, it is seen that throughput is always the same for MC-CDMA and DS-CDMA. In MC-CDMA, however, the throughput is different for different SF; the frequency diversity gain and the interference due to orthogonality distortion is higher for higher SF but the coding gain is higher for smaller SF due to better interleaving effect [21]. The detailed analysis of MC-CDMA system is out of the scope of this paper and left as an interesting future study.

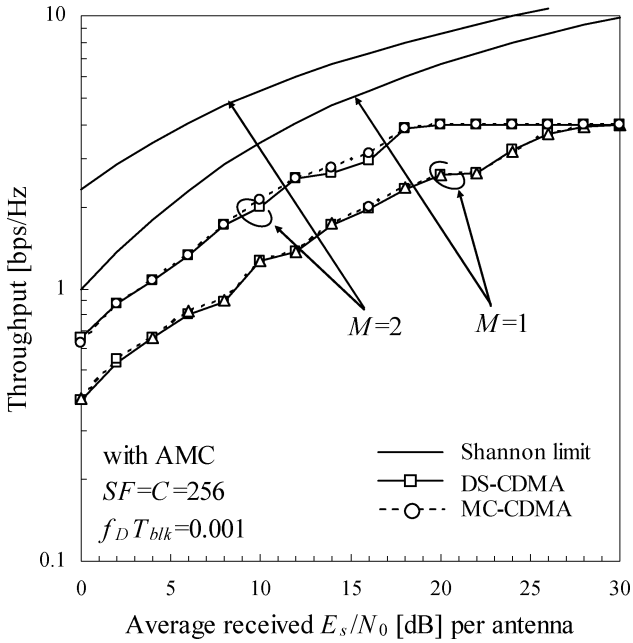

Fig. 10. Comparison with MC-CDMA.

For reference, the numerically evaluated Shannon limit is also plotted in Fig. 10 (the Shannon limit is given in Appendix). It is

seen that the calculated throughput follows the same trend but there is still much room for improvement. The throughput gap can be narrowed by the development of more efficient AMC and powerful HARQ protocol.

IV. Conclusion

In this paper, we showed that the use of MMSE-FDE for the reception of multicode DS-CDMA packet signal transmitted as in HSDPA gives an improved throughput. When Rake combining is used, the throughput degrades drastically with the increase in the frequency-selectivity of the channel due to orthogonality distortion among the orthogonal spreading codes. MMSE-FDE can replace Rake combining with much better throughput irrespective of the degree of channel frequency-selectivity except for the single-path channel (i.e., frequency-nonselective channel). It was found that with adaptive modulation and coding, there is a very small advantage of IR over CC employing frequency-domain packet combining based on MMSE criterion. It was also found that the same throughput can be achieved irrespective of the spreading factor for a full load condition. Also, shown was that the packet throughput of DS-CDMA with MMSE-FDE is the same as that of MC-CDMA.

In this paper, we have assumed ideal conditions since we intended to focus on evaluating the advantage of MMSE-FDE over the conventional Rake combining for packet transmissions. It is practically important to evaluate the performance under realistic conditions with chip synchronization, channel estimation and feedback channel error, and is left as an interesting future study.

Appendix

The standard formula for the Shannon capacity in a time-varying channel expressed in b/s/Hz is [22]

$$C = \log_2\left(1 + \Gamma|\xi|^2\right) \tag{A1}$$

where Γ is the average signal-to-noise power ratio and $|\xi|^2$ is the normalized channel power transfer function. In the case of a channel with L-independent identically distributed (i.i.d.) Rayleigh-faded paths having a uniform power delay profile and M receive antennas, the channel capacity is given by $C = \log_2(1 + \Gamma \cdot \chi)$, where $\chi = \sum_{m=0}^{M-1}\sum_{l=0}^{L-1}|\xi_{m,l}|^2$ with $E[|\xi_{m,l}|^2] = 1/L$. Hence, the average channel capacity $\overline{C}$ is given by

$$\overline{C} = \int_0^\infty \log_2(1+\Gamma\chi)p(\chi)d\chi \tag{A2}$$

where χ is chi-square distributed with $2ML$ degrees of freedom and its probability density function can be written as [23]

$$p(\chi) = \frac{L^{\mathrm{ML}}}{(\mathrm{ML}-1)!}\chi^{\mathrm{ML}-1}\exp(-L\chi). \tag{A3}$$

Substituting (A3) into (A2), the average channel capacity $\overline{C}$ can be numerically evaluated.

References

[1] F. Adachi, M. Sawahashi, and H. Suda, "Wideband DS-CDMA for next-generation mobile communications systems," *IEEE Commun. Mag.*, vol. 36, no. 9, pp. 56–69, Sep. 1998.

[2] 3GPP, High speed downlink packet access: Physical layer aspects, TR25.858, version 5.0.0.

[3] K. Tachikawa, "A perspective on the evolution of mobile communications," *IEEE Commun. Mag.*, vol. 41, no. 10, pp. 66–73, Oct. 2003.

[4] W. C. Jakes, Jr., Ed., *Microwave Mobile Communications*. New York: Wiley, 1974.

[5] K. Hooli, M. Latva-aho, and M. Juntti, "Multiple access interference suppression with linear chip equalizers in WCDMA downlink receivers," , Dec. 1999, pp. 467–471.

[6] G. E. Bottomley, T. Ottosson, and Y.-P. E. Wang, "A generalized RAKE receiver for interference suppression," *IEEE J. Sel. Areas Commun.*, vol. 18, no. 8, pp. 1536–1545, Aug. 2000.

[7] F. Adachi, T. Sao, and T. Itagaki, "Performance of multicode DS-CDMA using frequency domain equalization in a frequency selective fading channel," *Electron. Lett.*, vol. 39, no. 2, pp. 239–241, Jan. 2003.

[8] T. Itagaki and F. Adachi, "Joint frequency domain equalization and antenna diversity combining for orthogonal multicode DS-CDMA signal transmissions in a frequency selective fading channel," *IEICE Trans. Commun.*, vol. E87-B, no. 7, pp. 1954–1963, Jul. 2004.

[9] F. W. Vook, T. A. Thomas, and K. L. Baum, "Cyclix-prefix CDMA with antenna diversity," in *Proc. IEEE Veh. Technol. Conf.-Spring*, May 2002, pp. 1002–1006.

[10] I. Martoyo, T. Weiss, F. Capar, and F. K. Jondral, "Low complexity CDMA downlink receiver based on frequency domain equalization," in *Proc. IEEE Veh. Technol. Conf.-Fall*, Sep. 2003, pp. 987–991.

[11] I. Martoyo, G. M. A. Sessler, J. Luber, and F. K. Jondral, "Comparing equalizers and multiuser detectors for CDMA downlink systems," in *Proc. IEEE Veh. Technol. Conf.-Spring*, May 2004, pp. 1649–1653.

[12] K. L. Baum, T. A. Thomas, F. W. Vook, and V. Nangia, "Cyclic-prefix CDMA: An improved transmission method for broadband DS-CDMA cellular systems," in *Proc. IEEE Wireless Commun. Netwo. Conf.*, Mar. 2002, pp. 183–188.

[13] D. Chase, "Code combining—A maximum-likelihood decoding approach for combining an arbitrary number of noisy packets," *IEEE Trans. Commun.*, vol. 33, no. 5, pp. 385–393, May 1985.

[14] J. Hagenauer, "Rate-compatible punctured convolutional codes (RCPC codes) and their application," *IEEE Trans. Commun.*, vol. 36, no. 4, pp. 389–400, Apr. 1988.

[15] F. Adachi and S. Itoh, "Efficient ARQ with time diversity reception—Time diversity ARQ," *Electron. Lett.*, vol. 22, pp. 1254–1258, Nov. 1986.

[16] D. Falconer, S. L. Ariyavisitakul, A. Benyamin-Seeyar, and B. Eidson, "Frequency domain equalization for single-carrier broadband wireless systems," *IEEE Commun. Mag.*, vol. 40, no. 4, pp. 58–66, Apr. 2002.

[17] K. Takeda, T. Itagaki, and F. Adachi, "Joint use of frequency-domain equalization and transmit/receive antenna diversity for single carrier transmissions," *IEICE Trans. Commun.*, vol. E87-B, no. 7, pp. 1946–1953, Jul. 2004.

[18] A. Stefanov and T. Duman, "Turbo coded modulation for wireless communications with antenna diversity," in *Proc. IEEE Veh. Technol. Conf.-Fall*, Amsterdam, The Netherlands, Sep. 1999, pp. 1565–1569.

[19] F. Adachi and K. Takeda, "Bit error rate analysis of DS-CDMA with joint frequency-domain equalization and antenna diversity combining," *IEICE Trans. Commun.*, vol. E87-B, no. 10, Oct. 2004.

[20] N. Miki, H. Atarashi, S. Abeta, and M. Sawahashi, "Comparison of hybrid ARQ packet combining algorithm in high speed downlink packet access in a multipath fading channel," *IEICE Trans. Commun.*, vol. E85-A, no. 7, pp. 1557–1568, Jul. 2002.

[21] D. Garg and F. Adachi, "Diversity-coding-orthogonality trade-off for coded MC-CDMA with high level modulation," *IEICE Trans. Commun.*, vol. E88-B, no. 1, pp. 76–83, Jan. 2005.

[22] G. J. Foschini and M. J. Gans, "On limits of wireless communications in a fading environment when using multiple antennas," *Wireless Pers. Commun.*, vol. 6, no. 3, pp. 311–335, 1998.

[23] J. G. Proakis, *Digital Communications*, 3rd ed. New York: McGraw-Hill, 1995.

Deepshikha Garg received the M.E. and Dr. Eng. degrees in electrical and communications engineering from Tohoku University, Sendai, Japan, in 2002 and 2005, respectively.

Currently, she is with Kyocera Telecommunications Research Corporation, San Jose, CA. Her research interests include error control schemes, equalization, MIMO antenna systems including transmit/receive antenna diversity and accessing techniques for wireless communications.

Dr. Garg was the recipient of the 2002 Active Research Award in Radio Communication Systems from the Institute of Electrical, Information and Communication Engineers (IEICE) in 2002 and the YRP Young Researcher Award in 2003. She also received the Dean's Award from the School of Engineering, Tohoku University, for her Ph.D. dissertation.

Fumiyuki Adachi (M'79–SM'90–F'00) received the B.S. and Dr. Eng. degrees in electrical engineering from Tohoku University, Sendai, Japan, in 1973 and 1984, respectively.

In 1973, he joined the Electrical Communications Laboratories, Nippon Telegraph & Telephone Corporation (now NTT) and conducted various types of research related to digital cellular mobile communications. From 1984 to 1985, he was a U.K. SERC Visiting Research Fellow in the Department of Electrical Engineering and Electronics, Liverpool University. From July 1992 to December 1999, he was with NTT Mobile Communications Network, Inc. (now NTT DoCoMo, Inc.), where he led a research group on wideband/broadband CDMA wireless access for IMT-2000 and beyond. Since 2000, he has been with Tohoku University, where he is a Professor of Electrical and Communication Engineering at the Graduate School of Engineering. His research interests are in CDMA wireless access techniques, equalization, transmit/receive antenna diversity, MIMO, adaptive transmission, and channel coding, with particular application to broadband wireless communications systems.

Dr. Adachi is a member of the Institute of Electronics, Information and Communication Engineers of Japan (IEICE). He was a recipient of the Thomson Scientific Research Front Award in 2004, a corecipient of the IEEE VEHICULAR TECHNOLOGY TRANSACTIONS Best Paper of the Year Award in 1980 and 1990, a recipient of the Avant Garde Award in 2000, the IEICE Achievement Award in 2002, and a corecipient of the IEICE Transactions Best Paper of the Year Award in 1996 and 1998. He served as a Guest Editor for the IEEE JOURNAL ON SELECTED AREAS IN COMMUNICATIONS (Special Issue on Broadband Wireless Techniques, 1999, and for the Special Issue on Wideband CDMA I, 2000, and Wideband CDMA II, 2001).